EPJ Web of Conferences **163**, 00039 (2017) DOI: 10.1051/epjconf/201716300039
FUSION17

Study of Quasielastic scattering for ^{7}Li+^{159}Tb at around- barrier energies

A. Mukherjee[1,3,⋆], *Piyasi* Biswas[1,3], *Md. Moin* Shaikh[1], *Subinit* Roy[1,3], *A.* Goswami[1,3], *M.K.* Pradhan[1], *P.* Basu[1], *S.* Santra[2,3], *S.K.* Pandit[2,3], *K.* Mahata[2,3], and *A.* Shrivastava[2,3]

[1] *Saha Institute of Nuclear Physics, 1/AF Bidhannagar, Kolkata-700064, India*
[2] *Nuclear Physics Division, Bhabha Atomic Research Centre, Mumbai-400085, India*
[3] *Homi Bhabha National Institute, Anushaktinagar, Mumbai-400094, India*

Abstract. Quasielastic scattering cross sections for the reaction ^{7}Li+^{159}Tb have been measured at large back-angles, at energies around the Coulomb barrier. The quasielastic barrier distribution has been extracted from the measured quasielastic scattering excitation function, including and excluding α particle contribution. The peak of the quasielastic barrier distribution including α particle contribution shows a shift towards higher energy compared to the peak of the distribution without α particles. The quasielastic barrier distribution when compared to the calculated fusion barrier distribution, appears to show reasonable agreement for the system.

1 Introduction

Near barrier heavy ion fusion is strongly influenced by the internal structure of the colliding nuclei and coupling to the direct nuclear processes, like inelastic excitation and direct nucleon transfer. The coupling between the relative motion and intrinsic degrees of freedom of the interacting nuclei leads to an enhancement of fusion cross sections at energies below the average fusion barrier, relative to the cross sections obtained from the one-dimensional (1D) barrier penetration model calculations. The coupling essentially modifies the effective interaction potential and in turn splits the single, uncoupled fusion barrier into multiple barriers, thereby giving rise to a distribution of barriers.

It has been found that the nature of the couplings affecting the fusion process is not always apparent from the measured fusion cross sections. Rowley *et al.* proposed [1] a very sensitive approach for investigating the role of different couplings on the fusion cross sections at energies around the Coulomb barrier. The method consists in deriving the fusion barrier distribution (D_{fus}) from very precisely measured fusion cross sections, according to the prescription,

$$D_{fus}(E) = \frac{d^2}{dE^2}\left[E\sigma_{fus}(E)\right] \quad (1)$$

Over the past several years of research in heavy ion fusion, D_{fus} has been found to be a powerful tool to understand the effect of coupling of other channels on sub-barrier fusion and hence probe the reaction dynamics of nucleus-nucleus collision [2]. Since extraction of D_{fus} involves second derivative of $E\sigma_{fus}$, obtaining a meaningful barrier distribution requires very precisely measured fusion data.

⋆e-mail: anjali.mukherjee@saha.ac.in

Alternatively barrier distribution can also be obtained from large back-angle quasielastic (QEL) scattering excitation function [3]. QEL scattering is defined as the sum of elastic and inelastic scattering, transfer and other direct processes. Fusion is related to transmission through the barrier, whereas large back-angle QEL scattering is related to reflection at the barrier. Because of the conservation of reaction flux, these two processes may be considered as complementary to each other, and one may obtain information concerning one of them by investigating the other [3]. The barrier distribution of QEL scattering (D_{qel}) is obtained as [3],

$$D_{qel}(E) = -\frac{d}{dE}\left[\frac{d\sigma_{qel}}{d\sigma_{Ruth}}(E)\right] \quad (2)$$

As D_{qel} is derived from the first derivative, the uncertainty associated with D_{qel} extracted from back-angle QEL data is less than that associated with D_{fus}, which is extracted from the second derivative of fusion data. In view of the experimental benefits of D_{qel} over D_{fus}, the function D_{qel} may be considered to be a suitable alternative to D_{fus}.

Barrier distributions derived from the above two complementary approaches have been found to be similar for the systems where both the reactants are strongly bound [2, 4, 5]. In the past two decades, the influence of breakup of weakly bound projectiles, like ^{6,7}Li and ^{9}Be on fusion cross sections has been widely studied [6–9]. Some of these studies have been done with an aim to investigate the fusion barrier distributions for reactions with weakly bound projectiles on heavy targets [6]. Alongside, studies have also been carried out [10–16] to investigate the fusion barrier distributions derived from large back-angle QEL scattering cross sections for systems involving weakly bound nuclei. For such systems, the breakup channel is expected to play a significant role. For weakly bound

systems, QEL scattering, including no-capture breakup (NCBU) and incomplete fusion (ICF) along with elastic, inelastic and transfer processes, may be considered to be complementary to the complete fusion (CF) of the projectile with the target. For such systems, a comparative investigation of barrier distributions extracted from fusion and back-angle QEL excitation functions appears to be very interesting.

Recently, large back-angle QEL scattering cross sections have been measured for the ^{7}Li + ^{159}Tb system, at near-barrier energies. A preliminary analysis of the data have been done and QEL barrier distribution has been extracted from the QEL excitation function. Results of the preliminary analysis will be presented here.

2 Experiment and Analysis

Beams of ^{7}Li in the energy range 17−34 MeV, in steps of 1 MeV, delivered by the 14UD BARC-TIFR Pelletron Accelerator, Mumbai, India were used to impinge a self-supporting ^{159}Tb target foil of thickness ~ 1.1 $\mu g/cm^2$. To detect and identify the charged particles produced in the reaction a set of four ΔE-E telescopes of Si-surface barrier detectors were placed at $\pm 170^o$ and $\pm 160^o$, relative to the beam direction, inside a scattering chamber of diameter 1m. The thicknesses of the detectors were so chosen that the charged particles lose part of their kinetic energies in the first detector (ΔE) and stop in the second detector (E). However, the stop detectors used in the experiment were not thick enough to stop the Z=1 particles. Two Si-surface barrier detectors were placed at $\pm 20^o$ with respect to the beam direction for monitoring the beam and also for normalization purposes. In front of each telescope and monitor, a collimator was placed to define the solid angle. The energies of the incident beam were corrected for the loss of energy in the target material at half thickness of the target.

Figure 1(a) shows a typical two-dimensional ΔE-E_{tot} (where, E_{tot}=ΔE+E_{res}) spectrum obtained from the detector telescope taken at a scattering angle of $+170^o$. The events corresponding to (elastic + inelastic) scattering and various transfer or breakup products at E_{lab}=27 MeV are marked in the figure. The peak in the Z=3 band arises from contributions due to elastic scattering of ^{7}Li and inelastic scattering from the higher lying states of ^{159}Tb. The low lying levels of ^{159}Tb are very closely spaced and so the inelastic states of target could not be separated from the elastic events. The band may also contain contribution from the first inelastic state of ^{7}Li [14], if any. Besides, it may also contain the contribution from $^{6}Li_{g.s.}$, produced via n-stripping of ^{7}Li [14, 17]. It needs to be mentioned here that the events corresponding to ^{6}Li could not be separated from those of ^{7}Li in the spectra. However, the Z=3 band predominantly consists of elastic and inelastic events. So for nomenclature purpose, here we refer the Z=3 band as (elastic + inelastic) band. The Z=1 band shows a fall back feature because the stop detectors were not thick enough to stop the Z=1 particles. So the events corresponding to Z=1 could not be used in the analysis. The x-axis of the two-dimensional ΔE-E_{tot} spectrum was energy calibrated using the elastic peaks of ^{7}Li beam scattered from ^{159}Tb target at different bombarding energies below the Coulomb barrier.

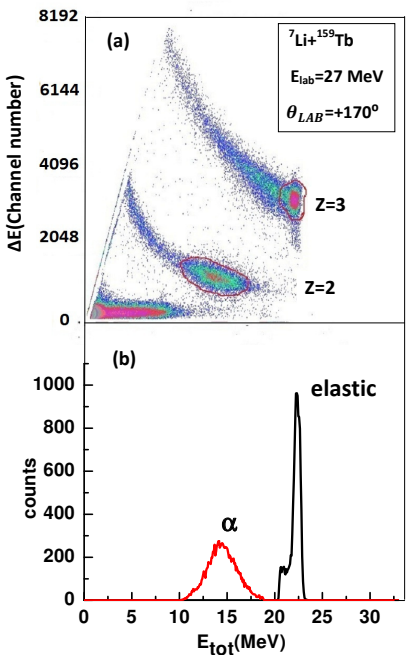

Figure 1. a) Typical ΔE-E_{tot} spectrum for the ^{7}Li+^{159}Tb reaction at E_{lab}=27 MeV and ΔE-E telescope angle of 170^o. b) A portion of the Z=3 and Z=2 projections on the ΔE-E_{tot} axis.

The x-axis projection of Z=3 (elastic + inelastic) band and Z=2 (α-particle) band, is shown in Fig. 1(b). The projection of Z=2 band shows a broad continuous peak with the centroid at around 14.5 MeV which is nearly equal to 4/7 times the incident beam energy. The contribution of the α-particles, emitted mostly at energies corresponding to the beam velocity primarily originate from breakup related processes, like NCBU (^{7}Li→ $\alpha + t$) and ICF (where t is captured by ^{159}Tb, following the breakup of ^{7}Li into $\alpha + t$). The broad α-peak can also have contributions from single nucleon transfer channels resulting in α-particles.

The ratio of quasielastic to Rutherford cross-sections is given by the expression,

$$\frac{d\sigma_{qel}}{d\sigma_{Ruth}}(E,\theta_{tel}) = \left[\frac{N_{qel}(E,\theta_{tel})}{N_m(E,\theta_m)}\right]\left[\frac{(d\sigma_{Ruth}/d\Omega)(E,\theta_m)}{(d\sigma_{Ruth}/d\Omega)(E,\theta_{tel})}\right] X \left(\frac{\Delta\Omega_m}{\Delta\Omega_{tel}}\right) \quad (3)$$

where, $N_{qel}(N_m)$ is the average yield in telescope (monitor) detector, $\frac{d\sigma_{Ruth}}{d\Omega}(E,\theta_m(\theta_{tel}))$ is the calculated Rutherford scattering cross-section at the corresponding bombarding energy E, at monitor angle θ_m (telescope angle θ_{tel}), and $(\frac{\Delta\Omega_m}{\Delta\Omega_{tel}})$ is the solid angle ratio of monitor to telescope

detector.

The $\frac{\Delta\Omega_m}{\Delta\Omega_{tel}}$ ratio was determined from the measurements at the lowest bombarding energies of 17, 18 and 19 MeV, where the elastic scattering is purely Rutherford. The ratio was estimated to be 0.0050 ± 0.00004. The Rutherford scattering cross section in the centre of mass frame is calculated using the formula,

$$\frac{d\sigma_{Ruth}}{d\Omega} = \frac{1}{16}\left(\frac{(z_a z_A e^2)^2}{(4\pi\epsilon_0)^2}\right)\frac{1}{E_{cm}^2 sin^4(\theta/2)} \quad (4)$$

where a and A refer to the projectile and target respectively.

At first, the "partial" QEL counts $N_{qel}(E,\theta_{tel})$ at each bombarding energy was obtained by selecting the region, marked in Fig. 1(a) of the Z=3 (elastic + inelastic) band. The area under the peak, marked "elastic" in Fig. 1(b), gives the value of $N_{qel}(E,\theta_{tel})$. As the measurements were done at angles less than 180^o, centrifugal correction was incorporated to obtain the effective c.m. energies. Figure 2(a) shows the "partial" QEL (elastic + inelastic) excitation function and the corresponding barrier distribution is shown in Fig. 2(b). Most of the error bars lie within the size of the data points.

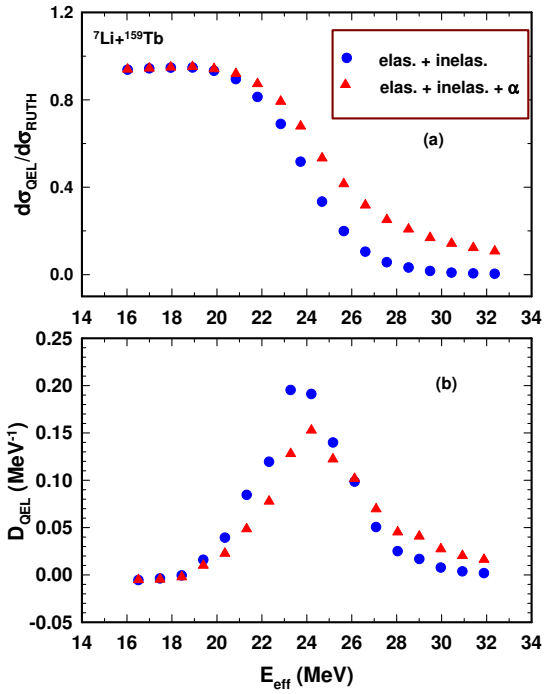

Figure 2. Comparison of a) quasielastic excitation function and b) quasielastic barrier distribution for ^{7}Li+^{159}Tb, excluding (•) and including (△) α particles.

Total QEL scattering cross sections is defined by adding the contribution of the α-particles to the above "partial" QEL scattering cross sections. For this, the α-particles shown in the marked region in Fig. 1(a) for the Z=2 band was considered. The area under the peak, marked "α" in Fig. 1(b), gives the contribution of the α particles. This when added to the Z=3 partial QEL scattered events gives the value of $N_{qel}(E,\theta_{tel})$, for determining the total QEL scattering cross sections. The experimental results of the total QEL scattering excitation function, including elastic, inelastic and α outgoing channels is shown in Fig. 2(a) and the corresponding QEL barrier distribution (D_{qel}) derived from the total QEL data is shown in Fig. 2(b). From Fig. 2(b) it can be observed that there is a shift in the peak of the barrier distribution when contribution of the α-particles is included in the QEL excitation function.

3 Discussion

It needs to be noted that this is an inclusive measurement and so the α-particle band will consist of α-particles produced in all possible ways in this reaction. In the ^{7}Li+^{159}Tb system, the compound nucleus evaporation α is expected to be negligible [7]. The processes that might contribute to the α- particle cross-sections for the ^{7}Li+^{159}Tb reaction are:
(1) NCBU: Breakup of ^{7}Li (B.U threshold for $\alpha + t$ is 2.46 MeV) into $\alpha + t$, either direct or sequential or both, where both the fragments escape without any being captured by the target
(2) Triton-ICF: t captured by the target following break up of ^{7}Li into $\alpha + t$ or a one step t-transfer to the target
(3) Neutron stripping: Single n-stripping from ^{7}Li will produce ^{6}Li which may break into $\alpha + d$ if excited above its breakup threshold 1.47 MeV
(4) Deuteron stripping: d-stripping from ^{7}Li will produce unbound ^{5}He that decays to α and a neutron
(5) Proton stripping: p-stripping from ^{7}Li will produce unbound ^{6}He which then decays to α and two neutrons
(6) Proton pickup: p-pickup by ^{7}Li will lead to ^{8}Be which immediately decays to two α-particles. Since this is an inclusive measurement, each ^{8}Be will contribute two α-particles to the total α-yield. But, the contribution of α-particles from the p-pickup may be expected to be very small compared to the total contribution of α-particles from other processes, like ICF (t+^{159}Tb) [17]. Hence, the extra α particle contribution arising from the double counting of the α-particles for the p-pickup channel may be neglected in comparison to the total α particle contribution for the reaction.
A comparison of the D_{qel}, including and excluding the α particle contribution, with the D_{fus} may shed some light on the importance of the α particle contribution in defining the QEL scattering events.

To compare D_{qel} with D_{fus}, an attempt was made to extract the D_{fus} from the measured fusion excitation function for ^{7}Li+^{159}Tb [7]. Unfortunately, D_{fus} could not be extracted from the reported fusion cross sections [7, 18], because only a few data points were available for differentiation. Therefore, a rough comparison of the experimental D_{qel} was made with the theoretical D_{fus}, extracted

from the fusion cross sections calculated using the coupled channels code, CCFULL [19]. All parameters were taken from Ref. [7]. In addition to the coupling scheme used in Ref.[7], here coupling to the first excited state of the projectile ^{7}Li, having spin $1/2^-$ (E_{ex}=0.477 MeV) with B(E2↑)=21.8 e^2fm^4 was also included using the rotational scheme [15], though it did not produce any appreciable change to the excitation function. It needs to be noted here that the CF cross sections for ^{7}Li+^{159}Tb at above barrier energies were seen to be suppressed by a factor of 0.74 [7]. The D_{fus} function in the present work was therefore extracted after multiplying the CC calculated CF cross sections by the factor of 0.74 [15]. To compare D_{qel} with D_{fus}, the D_{fus} values were normalized by $1/\pi R_b^2$, where the barrier radius R_b was taken from Ref. [7]. Figure 3 shows a comparison of the experimental D_{qel} with the theoretical D_{fus} (normalized). The dotted and the solid lines represent the D_{fus} obtained from the CC calculated fusion cross sections without and with coupling, respectively. The solid line can be seen to agree fairly well with the experimental D_{qel}, shown by the symbol △.

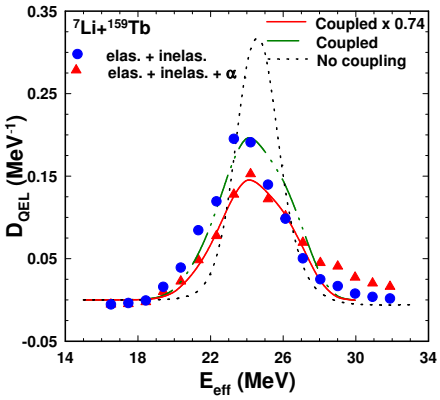

Figure 3. Comparison of the barrier distribution obtained from the quasielastic excitation function with and without inclusion of α particles for the system ^{7}Li+^{159}Tb. The dotted and the solid line represent the D_{fus} extracted from the CC calculated CF cross section without and with coupling, respectively. The calculated D_{fus} values have been normalized by the factor $1/(\pi R_b^2)$ to compare with D_{qel}. See text for details.

Thus, we see that the experimental D_{qel} including contribution of α particles agrees fairly well with the calculated D_{fus}. However, before reaching any definite conclusion, detailed analysis of the data need to be done and also the experimental D_{fus} for the system ^{7}Li+^{159}Tb has to be obtained.

4 Summary

The QEL excitation function for the system ^{7}Li+^{159}Tb has been measured at energies around the Coulomb barrier. The results of a preliminary analysis of the data have been presented at the conference. The D_{qel} functions have been extracted from the elastic + inelastic cross sections and also from the elastic + inelastic + α cross sections. Inclusion of α-particles shifts the D_{qel} peak towards the higher energy side. A rough comparison between the experimental D_{qel} and the calculated D_{fus} shows that the D_{qel} including the α-particle contribution agrees fairly well with the calculated D_{fus}. Detailed analysis of the data and measurement of the D_{fus} for the system ^{7}Li+^{159}Tb are necessary for a definite conclusion.

5 Acknowledgements

We sincerely thank the pelletron staff of BARC-TIFR, Mumbai for providing the beam. We would also like to thank Mr. Sujib Chandra Chatterjee of Saha Institute of Nuclear Physics for technical support during the experiment. One of the authors, Piyasi Biswas would like to thank the Council of Scientific & Industrial Research, India, for their financial support.

References

[1] N. Rowley, G.R. Satchler and P.H. Stelson Phys.A Lett. **B254**, 25 (1991)
[2] M. Dasgupta *et al.*, Annu. rev. Nucl. Part. Sci. **48**, 401 (1998) and references therein
[3] H. Timmers *et al.*, Nucl. Phys. **A584**, 190 (1995)
[4] H. Timmers *et al.*, Phys. Lett. **B399**, 35 (1997)
[5] H. Timmers *et al.*, Nucl. Phys. **A633**, 421 (1998)
[6] L.F. Canto *et al.*, Phys. Rep. **424**, 1 (2006), and references therein
[7] A. Mukherjee *et al.*, Phys. Lett. **B636**, 91 (2006), and
[8] M.K. Pradhan *et al.*, Phys. Rev. **C83**, 064606 (2011), and references therein
[9] Md. Moin Shaikh *et al.*, Phys. Rev. **C93**, 044616 (2016)
[10] C.J. Lin *et al.*, Nucl. Phys. **A787**, 281c (2007)
[11] J. Lubian *et al.*, Phys. Rev. **C78**, 064615 (2008)
[12] S. Mukherjee *et al.*, Phys. Rev. **C80**, 014607 (2009)
[13] D.S. Monteiro *et al.*, Phys. Rev. **C79**, 014601 (2009)
[14] M. Zadro *et al.*, Phys. Rev. **C87**, 054606 (2013), and references therein.
[15] C.S. Palshetkar *et al.*, Phys. Rev. **C89**, 024607 (2014)
[16] Md. Moin Shaikh *et al.*, Phys. Rev. **C91**, 034615 (2015)
[17] S.K. Pandit *et al.*, Phys. Rev. **C93**, 061602 (2016)
[18] R. Broda *et al.*, Nucl. Phys. **A248**, 356 (1975)
[19] K. Hagino, N. Rowley, and A.T. Kruppa, Comput. Phys. Commun. **123**, 143 (1999)